Light Scattering Study of Vitrification during the Polymerization of Model Epoxy Resins

Silvia Corezzi* and Daniele Fioretto

INFM and Dipartimento di Fisica dell'Università di Perugia, via Pascoli, 06123 Perugia, Italy

Debora Puglia and Josè M. Kenny

Materials Engineering Center, Università di Perugia, Loc. Pentima Bassa, 05100 Terni, Italy

Received December 31, 2002; Revised Manuscript Received May 13, 2003

ABSTRACT: The growth of macromolecules in reactive systems is associated with slowing down of the structural motions in a manner that closely resembles the effect of cooling or compressing glass-forming liquids. Depolarized photon correlation spectroscopy—which probes the molecular dynamics of a material via optical anisotropy fluctuations—has been used to monitor the reaction, at different temperatures, of three epoxy−amine formulations leading to network polymers via step-growth polymerization. The correlation function was fitted by the Kohlrausch−Williams−Watts form, and the parameters characterizing the structural relaxation process in the reactive mixtures were studied as a function of the extent of reaction, a quantity that was accurately measured by calorimetry. The behavior of the relaxation time successfully compares with a recently extended Adam−Gibbs entropy equation, derived from a connection between the reduction in configurations and the increase in number of chemical bonds during step polymerization.

I. Introduction

Glasses are amorphous solids: they have rigidity but lack long-range order. The ubiquity of these materials in nature and technology testifies to their importance. Notwithstanding, the process by which liquids turn into glasses partly remains an unsolved problem in condensed-matter physics.[1]

Glass formation entails slowing down continuously the particles in a liquid, to such an extent that the structure of the liquid no longer changes over the duration of a macroscopic experiment—say, 10^2 s. On this and shorter time scales the system is structurally arrested, while retaining topological disorder. Such a situation is commonly achieved in chemically stable liquids by reducing temperature or increasing pressure (physical vitrification); however, it may also be realized in chemically reactive systems due to progressive polymerization of the constituent molecules (chemical vitrification).[2] In the latter case, a correlation exists between the structural relaxation time τ and the extent of reaction resulting in a dynamical behavior very similar to that of systems undergoing physical vitrification. The similarity in the slowing down of dynamics of so different glass-formers as chemically stable liquids and irreversibly reacting mixtures is likely to originate in a basic, very general mechanism ruling structural rearrangement near the glass transition independent of the vitrification path. Explaining this similarity represents a crucial testing ground for theoretical models of the liquid−glass transition.

In front of many competing theories that claim success on the basis only of their ability to represent the temperature behavior of τ, pressure- and temperature-dependent experimental examinations favor the entropy theory,[3−6] in the form of the Adam and Gibbs equation,[7] as a pretender to a coherent theoretical description of liquid−glass transition phenomena. The entropy viewpoint intuitively adapts to polymerization processes, where formation of covalent bonds in place of weaker interactions between molecules should decrease the system's configurational entropy S_c and correspondingly increase the relaxation time τ. Although intuitive, such a conjecture is not proven so far but only taken for granted. Johari and co-workers,[8−10] for example, assumed the Adam and Gibbs equation to be valid and combined it with a phenomenological function they chose to describe the dependence of τ on the extent of reaction. Matsuoka and co-workers[11] employed the Adam and Gibbs equation in modeling epoxy cure by assuming without argument that the temperature where S_c vanishes varies linearly with extent of reaction.

A direct proof of the entropy theory in chemical vitrification needs parallel information on how τ and S_c change throughout a reaction. Unfortunately, the character of the process prevents from doing an experimental determination of S_c as the difference of total and vibrational entropy—even an estimate of S_c as excess entropy of the liquid over the glass is impossible in a direct manner[12]—and demands finding an alternative method. A way to proceed is using physical arguments to connect the reduction in configurational entropy during reaction with a measurable chemical variable, so as to change the original Adam and Gibbs equation into a relation that can be tested between the structural relaxation time and a quantity experimentally accessible. We show in section II the case of step polymerization reactions, in which the derived equation lends itself to stringent experimental tests due to very strong and somehow surprising predictions. The model equation was recently tested on two epoxy-curing processes, both monitored by means of dielectric spectroscopy.[6] Here we report a study of six epoxy-curing reactions, monitored by depolarized photon correlation spectros-

* To whom correspondence should be addressed. E-mail: Silvia.Corezzi@fisica.unipg.it.

10.1021/ma026021q CCC: $25.00
Published on Web 06/14/2003

copy in combination with standard calorimetry, to test the entropy model predictions in a broader condition range. The results of the study are presented and discussed in sections III and IV, respectively.

The curing of epoxy-based thermosets represents a chemical vitrification process of primary technological importance, which has been studied to various extents by a number of experimental techniques, e.g., dielectric,[6,8−10,13−26] light scattering,[17,27−30] heat capacity,[31,32] and infrared[18,33−35] spectroscopies and rheological,[36,37] calorimetric,[8,10,19−21,26,38−40] and ultrasonic[29,34,41] methods. Because of the broad time range investigated (ranging from picoseconds to hundreds of seconds), light scattering and dielectric spectroscopy are the most valuable techniques for studying dynamics near the glass transition. The former, however, although widely used in physical vitrification, has not as widely been used to monitor the hardening process of epoxy thermosets. In particular, Brillouin scattering spectroscopy has been used[28−30] to probe collective dynamics in the short-time (i.e., high-frequency) range selected by gratings and Fabry−Perot interferometers. By contrast, attempts to apply photon correlation spectroscopy (PCS) to probe the long-time (i.e., low-frequency) dynamics in these systems are relatively recent.[17]

Light is scattered as a result of fluctuations in the dielectric tensor of a liquid, to which contribute different microscopic mechanisms: thermally activated density fluctuations, concentrations fluctuations (if the sample is not homogeneous), and anisotropy fluctuations (if the molecules are optically anisotropic). Light scattering techniques gain access differently to the dynamics of these fluctuations, depending on the interaction geometry: polarized scattering techniques reveal density, concentration, and anisotropy fluctuations; depolarized techniques are only revealing for anisotropy fluctuations.[42] If the scattered light is not analyzed for polarization (unpolarized scattering technique), then polarized and depolarized signals superimpose.

In polymerization studies, unpolarized PCS was recently applied by Fitz and Mijovic[17] to investigate a chemically reactive network-forming system (diglycidyl ether of bisphenol A cured with diethylenetriamine in stoichiometric amount). Unpolarized and depolarized PCS was employed to follow chain polymerization of bulk styrene by Stevens and co-workers[43,44] and by Chu and Fytas.[45] To our knowledge, however, there have been no studies of step polymerization by depolarized PCS. This article presents the first successful application of this technique to the study of dynamics in network-forming systems near the glass transition. Also, on approaching the glass transition, both fluctuations in density and optical anisotropy are slow enough to be observed by PCS.[46] By measuring the correlation function of anisotropy fluctuations only, we take advantage of the absence of distortions that could arise from simultaneous contributions from density fluctuations.

II. Theoretical Basis

One way of rationalizing the qualitative notion, implied by Kauzmann's[47] observation of paradoxical entropy loss upon supercooling, of a connection between dynamics and thermodynamics in liquids approaching the glass transition is in terms of the model of Adam and Gibbs.[7] The theory links the structural relaxation time τ and the configurational entropy S_c of a liquid via

$$\tau = \tau_0 \exp(C/TS_c) \tag{1}$$

with τ_0 and C nearly constant. The extent to which results of experimental studies performed by varying temperature[48] and pressure[4−6] and results of computer simulations at different temperatures and densities[49,50] agree with eq 1 even goes beyond what would be expected from a crude model, as the entropy theory seems to be. Here we show that a relation can be derived from eq 1 also to describe the evolution of the structural relaxation time during chemical vitrification. The conditions for such a relation are sufficiently simplified to ensure minimum formal complexity but still sufficiently general to be approximately met by many real systems.

An entropy-based picture would qualitatively apply to polymerization reactions, if the relaxation rate is higher than the rate of reaction, so that the system experiences a succession of quasi-equilibrium states. In the entropy view, a dearth of available configurations, progressively reduced by new covalent bonds, expresses itself in the cooperative motion of the system, in such a way that the lower the configurational entropy, the greater the size of the cooperatively rearranging regions (CRRs). It is not obvious, in general, how to relate a decrease in configurational entropy to the advancement of reaction by a measurable chemical parameter. In step polymerization,[51] however, configurational entropy can be related to chemical conversion, $\alpha(t)$, which measures the extent of reaction through the fraction α of functional groups that have reacted at elapsed time t since the beginning. Owing to the random nature of the step-growth mechanism, the degree of polymerization increases steadily throughout the reaction, but neither long chains nor large networks are formed on average until very high conversions are reached, even though the monomer is rapidly consumed in the early stages of the reaction. In such a situation, at any fixed temperature, one can expect monomers linked with each other approximately to behave as a single cooperative unit. As they are interlocked segments, a change in configuration of any one of them causes a change in configuration of the others, and it is realistic to expect that the average number of different configurations accessible to one cooperative region remains the same. This argument can be formalized in $W_c(\alpha) = W_c(0)^{1/x_n}$, where x_n is the number-average degree of polymerization (i.e., the average number of monomers per molecule), $W_c(\alpha)$ is the number of configurations available to the macroscopic system at conversion α, and $W_c(0)$ is the number of configurations at $\alpha = 0$. Accordingly, for the configurational entropy one has

$$S_c(\alpha) = S_c(0)/x_n \tag{2}$$

In the Adam−Gibbs formalism (where the CRRs' size relates inversely to S_c),[7] eq 2 asserts that the CRRs' size grows in proportion to the average size of the molecules comprising the system, which is believable under the conditions described above.

Simple considerations allow one to predict the dependence of x_n on α. For the general system consisting of a mixture of N_A moles of monomers each bearing f_A functional groups of type A, together with N_B moles of monomers with f_B functional groups of type B (where the A groups can react only with B groups and vice versa), provided that no rings are formed, x_n can always be obtained by elementary stoichiometry[52,53] as

$$x_n(\alpha_A) = 1/(1 - \langle f_A\rangle\alpha_A) \quad (3)$$

where α_A is the fraction of A groups that have reacted and $\langle f_A\rangle = N_A f_A/(N_A + N_B)$ is the average number of A groups per monomer initially present in the mixture. (Similar relations hold with B replacing A; hence, the subscript will be omitted from now on for simplicity of notation, by keeping in mind that $\langle f\rangle$ and α must refer to the same kind of functional group.) Thereby, one has $S_c(\alpha) = S_c(0)(1 - \langle f\rangle\alpha)$—that is, a linear dependence of S_c on α—which translates eq 1 into

$$\tau = \tau_0 \exp\left(\frac{B(T)}{1 - \langle f\rangle\alpha}\right) \quad (4)$$

with τ_0 approximately independent of both T and α, and $B(T) = [C/TS_c(0)]$ only dependent on temperature, on the reasonable assumption that the variation of C with α is negligible.

Very strong predictions follow from eq 4: first, the structural relaxation time diverges ("ideal" glass transition) when α equals the theoretical value $\alpha_0^{theor} \equiv 1/\langle f\rangle$; second, because the system's average functionality $\langle f\rangle$ may be tuned by varying the molar ratio of reagents, α_0^{theor} can also be controlled in the same way, independent of the reaction details and temperature.

III. Experimental Section

Materials. We studied three epoxy−amine formulations, during isothermal reactions yielding network polymers. Two epoxy prepolymers (diglycidyl ether of bisphenol A ≡ DGEBA) were used, with functionality $f = 2$ and slightly different epoxy equivalent weights: EPON828 by Shell (eew = 190) and DGEBA348 by Aldrich (eew = 174). EPON828 was cured with ethylenediamine (EDA, by Aldrich; $f = 4$) in the 2:1 and 1:1 molar ratio, so as to realize both stoichiometric and nonstoichiometric balance of mutually reactive functional groups; DGEBA348 was cured with diethylenetriamine (DETA, by Aldrich; $f = 5$) in the molar ratio of 4:3. All materials were used as received. Each mixture was prepared by mixing for 2−3 min and then transferred into the measurement cell. As known, the reactions proceed via polyaddition. The molar ratios of reagents where chosen in order to have systems with very different average epoxy functionality $\langle f\rangle$ and accordingly different α_0^{theor} as follows: $\alpha_0^{theor} = 1.00$ in EPON828/EDA 1:1, $\alpha_0^{theor} = 0.88$ in DGEBA348/DETA 4:3, and $\alpha_0^{theor} = 0.75$ in EPON828/EDA 2:1.

Calorimetry. For each reaction, the chemical conversion of epoxy groups has been determined as a function of the reaction time by calorimetry. Data are partly taken from the literature partly unpublished. Epoxy conversion during isothermal cure of DGEBA348/DETA 4:3 is obtained from new measurements. The heat flow released during isothermal runs (Figure 1a) and during dynamic runs at constant heating rates (+5, +10, and +15 °C/min; from −40 to +200 °C) was acquired by a Perkin-Elmer Pyris 1 calorimeter. The conversion, α, at any time t during isothermal reaction can be calculated as

$$\alpha(t) = \frac{\int_0^t \frac{dH}{dt}\,dt}{\Delta H_T} \quad (5)$$

where the numerator is the heat released isothermally until time t, $\Delta H_{iso}(t)$, and ΔH_T is the total heat of reaction calculated by integration of the total area enclosed under a dynamic thermogram. ΔH_T can also be obtained by $\Delta H_T = \Delta H_{iso} + \Delta H_{res}$, with ΔH_{res} the residual heat evolved during a subsequent postcure dynamic scanning.[39,54] In our case, the values of ΔH_T determined with the two methods agreed within the experimental error. Discrepancies are normally expected for processes conducted at high temperatures where a considerable uncertainty affects the determination of heat evolved during the initial part of the isothermal peak. Figure 1b shows the $\alpha(t)$ profiles for the DGEBA348/DETA 4:3 system at $T = 50$, 30, and 25 °C.

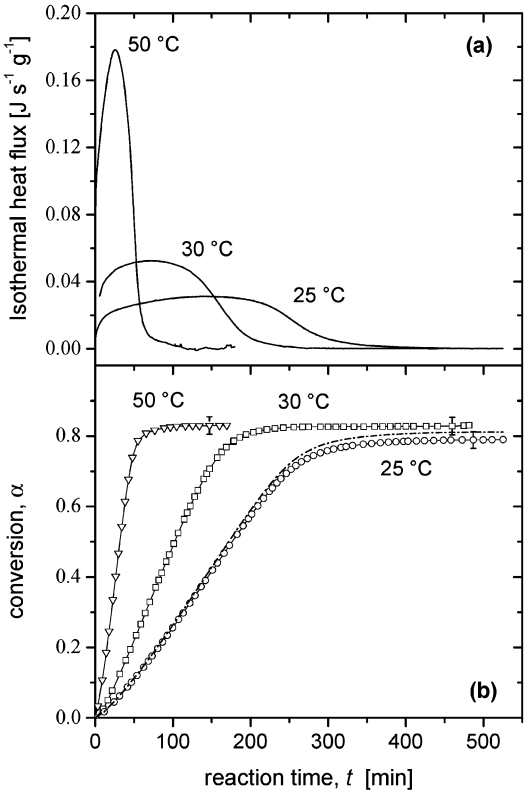

Figure 1. (a) Heat flow per gram of mixture released during isothermal cure of DGEBA348/DETA 4:3 at 50 °C (sample of 13.1 mg), 30 °C (sample of 15.6 mg), and 25 °C (sample of 10.1 mg) vs the reaction time, t. (b) Calorimetric conversion of epoxy groups, α, as a function of the reaction time. Open symbols are obtained with $\Delta H_T = 580 \pm 12$ J/g, calculated from seven independent dynamic runs. The dash−dot curve is obtained with $\Delta H_T = 564$ J/g, calculated by summing the isothermal and postcuring heats of the sample cured at 25 °C. Error bars represent an uncertainty of 3%, arising from an error of 2% estimated on ΔH_T and an error of 1% on the sample weight.

For the EPON828/EDA 2:1 system, $\alpha(t)$ at 25 °C is taken from ref 18; at 23 and 32.1 °C, instead, it was obtained by combining the $\Delta H_{iso}(t)$ from ref 20, with the value $\Delta H_T = 230.5$ kJ/mol of EPON828 given in ref 19. Determination of $\alpha(t)$ for the EPON828/EDA 1:1 system at 25 °C is reported in ref 21.

Photon Correlation Spectroscopy (PCS). A fresh reactive mixture was prepared for each PCS experiment and strained into a dust-free cylindrical cell of 10 mm o.d. The temperature of the sample holder was controlled within ±0.1 °C throughout the reactions. Measurements were performed in the homodyne mode. The incident light was generated by a single mode diod-pumped solid-state laser operating at λ = 532 nm and was vertically polarized (i.e., polarized perpendicular to the scattering plane). The horizontally polarized scattered light (VH configuration) was collected at an angle $\theta = 90°$ in the scattering plane and analyzed by a Brookhaven BI-9000AT digital correlator. Depolarized correlation functions (d-PCS spectra) were obtained in the time range 10 μs−10 s during the following reactions: EPON828/EDA 1:1 at 25 °C; EPON828/EDA 2:1 at 23, 25, and 32.1 °C; DGEBA348/DETA 4:3 at 25 and 30 °C. The 2 mm diameter laser beam was sent through the sample without focusing on it to avoid local heating that would speed the reaction up and even induce macroscopic bubbles. Preliminary tests showed no appreciable dependence of the spectra on the laser power up to a maximum value of 200 mW, used in all the experiments. The acquisition time for each spectrum was set short enough for the system

to be considered in equilibrium and long enough for the signal-to-noise ratio to be reasonable. Depending on the reaction, we used acquisition times of 1−2 min. A similar compromise could not be reached in the DGEBA348/DETA 4:3 system at 50 °C because the reaction takes less than 1 h to reach completion (see Figure 1).

Depolarized light scattering presents some advantages in following polymerizations. First, the depolarized technique bypasses some problems connected to the presence in the sample of small air bubbles formed during the mixing of the reagents. In fact, the strong contribution of light elastically scattered from bubbles has a large polarized component that disturbs VV correlation functions, especially at long correlation times. On the other hand, in the VH configuration, that contribution is considerably depressed, and the signal-to-noise ratio does not get worse significantly. Second, the depolarized light scattering spectra, different from the polarized and unpolarized ones, only receive contribution from fluctuations in the off-diagonal components of the optical polarizability tensor (optical anisotropy fluctuations)[42] and hence only reflect orientational dynamics of the molecules. Density fluctuations, associated with translational modes, do not contribute to the processes observed in depolarized spectra, unless a strong translation−rotation coupling exists. On the basis of results from recent studies, which found a negligible coupling in DGEBA[55] and other materials,[56,57] we infer that depolarized scattering in the present experiments on DGEBA/aliphatic-amine mixtures is dominated by optical anisotropy fluctuations due to collective reorientation fluctuations of the units of the fluid. Also, since the technique probes the dynamics of anisotropy fluctuations only, the difficulties of data analysis connected with the distinction in the correlation function of other contributions (from density and concentration fluctuations) that may enter the experimental time window of the photon correlator[17,43] are directly overcome.[44]

Data Analysis and Results. PCS in the homodyne mode measures the light intensity autocorrelation function, i.e., the quantity $G^{(2)}(\tau) \equiv \langle I(\tau)I(0)\rangle$, where τ denotes the correlation time and the brackets indicate a time average.[42] For a Gaussian random process, $G^{(2)}(\tau)$ is related to the autocorrelation function of the scattered field $g^{(1)}(\tau) \equiv \langle E(\tau)E(0)\rangle/\langle|E(0)|^2\rangle$ via

$$G^{(2)}(\tau) = \langle I\rangle^2(1 + F|g^{(1)}(\tau)|^2) \qquad (6)$$

where F is an instrumental factor of the order of unity. The relaxation function for processes observed in highly viscous system is generally more stretched than a single-exponential decay; we then use the Kohlrausch−Williams−Watts (KWW) function to account for the time decay of $g^{(1)}(\tau)$:

$$g^{(1)}(\tau) = a\ \exp[-(\tau/\tau_K)^{\beta_K}] \qquad (7)$$

There, a is the fraction of the total scattered light which is scattered via anisotropy fluctuations involved in the structural relaxation, the stretching parameter $0 < \beta_K \leq 1$ quantifies the deviation from single-exponential behavior, and τ_K is a measure of the characteristic time of the process, connected to the average relaxation time $\langle\tau\rangle$ by the relationship $\langle\tau\rangle = \Gamma(\beta_K^{-1})\tau_K/\beta_K$, with Γ the Eulero gamma function.

Typical d-PCS spectra (symbols) at different reaction times, and their fit by using eqs 6 and 7 (solid lines), are represented in a normalized fashion in Figure 2 for DGEBA348/DETA 4:3 at 25 and 30 °C and in Figure 3 for EPON828/EDA 2:1 and EPON828/EDA 1:1 at 25 °C. By changing the reaction time t into chemical conversion α through the $\alpha(t)$ calorimetric curves (e.g., Figure 1), the evolution of the structural relaxation process can then be described in terms of the dependence on conversion of τ_K, β_K, $\langle I\rangle^2$, and Fa^2. Figures 4−6 show such dependence during the reaction of DGEBA348/DETA 4:3. The $\tau_K(\alpha)$ behavior in the EPON828/EDA 1:1 and EPON828/EDA 2:1 systems is displayed in Figure 7. The results of Figures 6 and 7, in particular, will be discussed in section IV.

The anisotropy fluctuations should relax much faster than 10^{-5} s in the early stage of reaction. As expected, Figures 2 and 3 show that the correlation function of anisotropy fluctuations enters the time window of the present photon correlator from a reaction time that corresponds to relatively high conversion. Because of the limited time window, it could not be possible to leave all the parameters free in the fit of all the spectra, but it was possible in the fit of the spectra with an associated time scale that falls well inside the autocorrelation time window. In these latter, we found that both the amplitude and the shape of the correlation function were almost constant as the reaction proceeded. In particular, the values of β_K

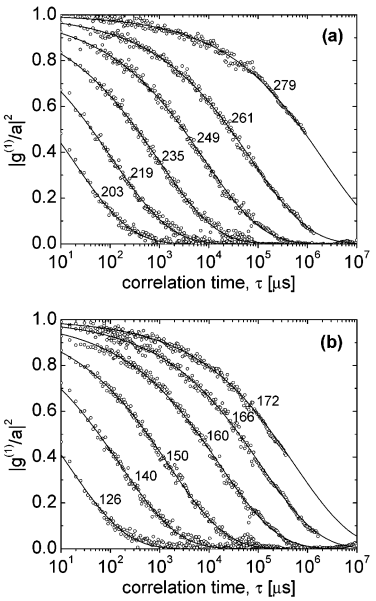

Figure 2. Depolarized photon correlation spectra of DGEBA348/DETA 4:3, taken at different reaction times during isothermal reaction (a) at $T = 25$ °C and (b) $T = 30$ °C. The acquisition time of each spectrum was 120 s at 25 °C and 60 s at 30 °C. Numbers indicate the reaction time, in minutes. Solid lines are the best fit using eqs 6 and 7.

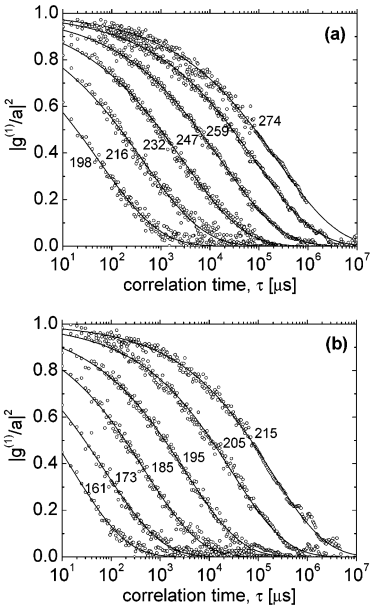

Figure 3. (a) Depolarized photon correlation spectra of EPON828/EDA 2:1, taken at different reaction times during isothermal reaction at $T = 25$ °C. The acquisition time of the spectra was ranging between 60 and 120 s. (b) Depolarized photon correlation spectra of EPON828/EDA 1:1, taken at different reaction times during isothermal reaction at $T = 25$ °C. Each spectrum was acquired in 60 s. Numbers indicate the reaction time, in minutes. Solid lines are the best fit using eqs 6 and 7.

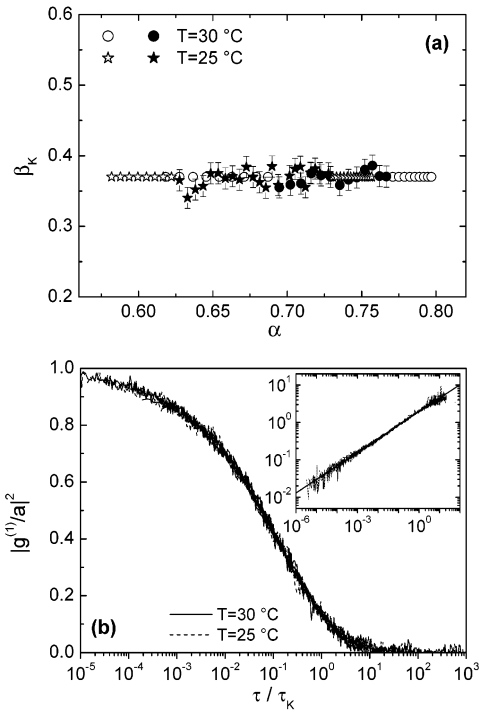

Figure 4. (a) Stretching parameter, β_K, during reaction of DGEBA348/DETA 4:3, reported as a function of the epoxy conversion α. Closed symbols indicate that β_K was acting as free parameter in the fit, and open symbols indicate that β_K was fixed. (b) Master plot of the normalized spectra at different times during reaction of DGEBA348/DETA 4:3 at $T = 25$ and 30 °C. The spectra are the same as in Figure 2. In the inset: master plot obtained by replotting the data in the form $-\ln(|g^{(1)}(\tau)/a|^2)$ vs τ/τ_K on a double-logarithmic scale. The data collapse into a single line with slope $\beta_K = 0.37$ (solid line).

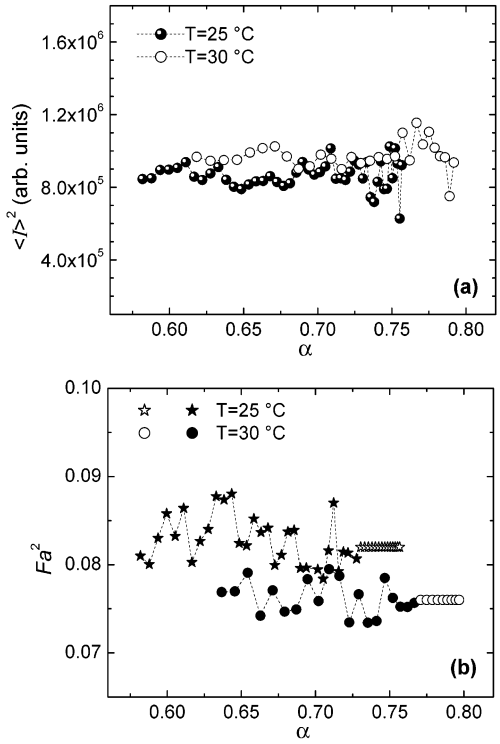

Figure 5. (a) Square of the average light intensity, $\langle I \rangle^2$, detected in the PCS experiments on DGEBA348/DETA 4:3, reported as a function of the epoxy conversion α. (b) Intensity ratio, Fa^2, as a function of the epoxy conversion α. Closed symbols indicate that Fa^2 was acting as free parameter in the fit, and open symbols indicate that Fa^2 was fixed.

observed in the present experiments were near 0.4 and, for any mixture, independent of the reaction temperature (namely, it was $\beta_K = 0.37 \pm 0.02$ in DGEBA348/DETA 4:3, $\beta_K = 0.40 \pm 0.02$ in EPON828/EDA 1:1, and $\beta_K = 0.35 \pm 0.02$ in EPON828/EDA 2:1). Assuming the validity of a time−conversion superposition principle, at least over the conversion range covered by the present study, we were able to extend the fit to those spectra where only a portion of the relaxation region is observed inside the autocorrelation time window. As an example, in the case of DGEBA348/DETA 4:3, the fit parameters taken as fixed in the fit of the spectra are marked with open symbols in Figures 4a and 5b, and additional verification of a KWW form of the spectra with constant shape in the conversion range investigated is provided in Figure 4b. There, the data collected at different reaction times and temperatures are shown to collapse into a single master curve by replotting the normalized correlation function vs the normalized relaxation time. In the inset of Figure 4b we apply an alternative graphical method which emphasizes the agreement with the form of a single KWW function, based on the observation that eq 7 yields a straight line when it is plotted as $\log[-\ln(g^{(1)}(\tau)/a)]$ vs $\log \tau/\tau_K$, with slope equal to β_K.

The fit procedure described here provided in all the systems reliable values for the relaxation time over 4 decades or more, for times $>10^{-4}$ s. These data are our present basis for a deeper discussion of the dynamics in chemically vitrifying systems.

IV. Discussion

In this section, we focus on the simple relation (eq 4) predicted by the reaction-extended entropy model. However crude the underlying picture may appear, we think that it is not cruder than the entropy theory itself: the most severe test will be a comparison with experimental results. In Figures 6 and 7 the relaxation

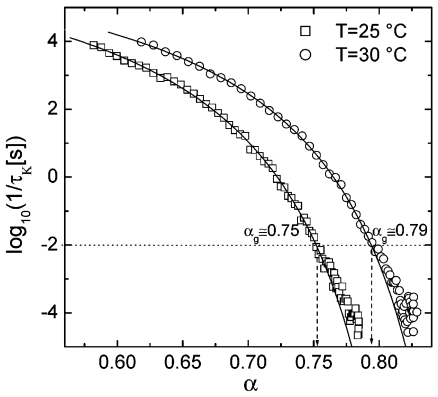

Figure 6. Structural relaxation time, τ_K, of DGEBA348/DETA 4:3 at 25 and 30 °C as a function of the epoxide conversion, α. The solid lines, whose parameters are listed in Table 1, represent the best fit with eq 4. The dotted horizontal line indicates the glass transition point, operationally defined by $\tau_K(\alpha_g) \approx 10^2$ s.

time behavior measured by depolarized PCS is displayed as $\log(1/\tau_K)$ vs α. This plot, drawn in strict analogy to the most familiar Arrhenius plot which is usual in the temperature domain, highlights the similarity in the evolution of the structural relaxation time during polymerization with the evolution due to temperature or pressure variations.

Step polymerizations of epoxy−amine systems such as those considered in the present study are expected, in a good approximation, to fulfill the requirements for application of eq 4: (i) tendency to cyclization (i.e., ring formation) is known[58] to be negligible in the curing of DGEBA with amines, owing to the large distance between the epoxy groups and the rigidity of the

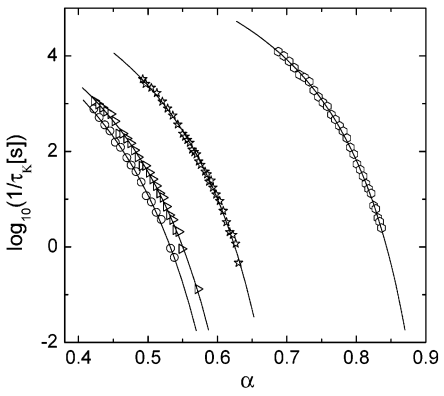

Figure 7. Structural relaxation time, τ_K, of EPON828/EDA 1:1 at 25 °C (hexagons), EPON828/EDA 2:1 at 25 °C (stars), EPON828/EDA 2:1 at 23 °C (triangles), and EPON828/EDA 2:1 at 32.1 °C (circles) as a function of the epoxide conversion, α. The solid lines, whose parameters are listed in Table 1, represent the best fit with eq 4.

Table 1. Best-Fit Parameters Obtained by Using Eq 4 To Fit the Dependence on Conversion, α, of the Structural Relaxation Time, τ_K, of Polymerizing Systems during Isothermal Reaction at Temperature *T*

system	*T* [°C]	$1/\langle f\rangle^a$	log τ_0^{-1} [s^{-1}]	B
EPON828/EDA 1:1	25	1.00 ± 0.03	7.8 ± 0.3	2.7 ± 0.3
DGEBA348/DETA 4:3	25	0.87 ± 0.02	7.9 ± 0.2	3.1 ± 0.2
DGEBA348/DETA 4:3	30	0.90 ± 0.02	7.8 ± 0.2	2.8 ± 0.2
EPON828/EDA 2:1	23	0.76 ± 0.03	8.4 ± 0.7	5.3 ± 0.9
EPON828/EDA 2:1	25	0.80 ± 0.03	8.4 ± 0.4	4.3 ± 0.4
EPON828/EDA 2:1	32.1	0.75 ± 0.01	8.4 (fixed)	5.5 ± 0.2

[a] The values $1/\langle f\rangle$ obtained experimentally must be compared with the values α_0^{theor} predicted theoretically, which are $\alpha_0^{theor} = 1.00$ (for 1:1 mixture), $\alpha_0^{theor} = 0.88$ (for 4:3 mixtures), and $\alpha_0^{theor} = 0.75$ (for 2:1 mixtures). For a given reaction, the same $1/\langle f\rangle$ is expected for different *T*. An uncertainty of the order of 2−3% is due to errors inherent in the experimental determination of chemical conversion.

DGEBA molecule; (ii) in the investigated conversion range the probability that long chains or large cross-linked structures are formed is relatively small.[53,59−62] Moreover, for each mixture, the reaction temperature was set so as to make the system's reactivity sufficiently low. As previously mentioned, the reactions studied can be divided into three groups, depending on the average epoxy functionality of the system, $\langle f\rangle$. The stoichiometries adopted here are such that the following three distinct values are realized: $\langle f\rangle = 1/1$, 8/7, and 4/3, corresponding to $\alpha_0^{theor} = 1.00$, 0.88, and 0.75, respectively.

For each isothermal reaction the relaxation time behavior is fitted by eq 4, with τ_0, *B*, and $\langle f\rangle$ as free parameters. The fit parameters are listed in Table 1, and the corresponding curves are drawn in Figures 6 and 7 with solid lines. It should be noted that the fit is performed only to experimental data such that $\log(1/\tau_K) > 0$, obtained from correlation spectra well inside the experimental time window. Remarkably, the results in Table 1 meet our expectations for the values of the fit parameters. In particular, in all cases examined the divergence of τ_K occurs, within quite acceptable experimental error, strictly around the ideal values α_0^{theor} that are expected for our mixtures solely on the basis of their functionality and molar ratios, independent of *T*. This astonishing result constitutes a strong evidence in favor of eq 4. In particular, it supports the connection we made between the reduction in configurational entropy and the amount of chemical bonds during step polymerization (eqs 2 and 3); also, it demonstrates that a Vogel−Fulcher-like dependence on conversion for the structural relaxation time, proposed by different authors on a phenomenological basis[22,23,26] or a semiempirical $T_g(\alpha)$-based approach,[63−65] originates in the Adam−Gibbs entropy equation. In this frame, the conversion where the structural relaxation time would ideally diverge is the conversion at which the configurational entropy of the system tends to vanish, whose value under the above-mentioned conditions is predictable.

A check of consistency on eq 4 comes from the temperature dependence of its parameters. The *T* dependence of the preexponential factor τ_0 is expected to be negligible and that of the *B* parameter to be related to that of $S_c(0)$ and *C*. The variation with *T* of $S_c(0)$ reasonably overwhelms the variation of *C*, related to a rearranging unit's activation free energy, and can be expressed as $S_c(0;T) = \int_{T_0}^{T}(\Delta C_p/T'\,dT')$, with ΔC_p the configurational heat capacity and T_0 the ideal glass transition temperature of the unreacted mixture. By the usual approximation $\Delta C_p \propto 1/T$,[48] $B(T)$ takes the form $B(T) = D/(T - T_0)$ with *D* a constant (yielding a Vogel−Fulcher temperature dependence of τ at any fixed conversion). We note that the experimental values of τ_0 and *B* are consistent with the expected temperature trends. This result can be better appreciated in ref 66 on the basis of more data obtained by dielectric spectroscopy.

It is now worth mentioning several consequences of eq 4. First, a decreasing linear behavior with α of the "kinetic fragility", quantified by the index K_{VFT} in the Vogel−Fulcher equation written as $\tau = \tau_0 \exp\{1/[K_{VFT}(T/T_0 - 1)]\}$, is implicit in eq 4. In fact, using $B(T) = D/(T - T_0)$, it is possible to turn the equation into the mentioned Vogel−Fulcher form with the fragility index given by

$$K_{VFT} = (T_0/D)[1 - \langle f\rangle\alpha] \tag{8}$$

This behavior for the evolution of fragility in step-polymerizing systems, in which covalent bonds progressively replace van der Waals or H-bonds, is consistent with the presence of an increasing fraction of highly directional interactions between molecules, as typical of "strong" systems.[67] Although the character of the reaction makes an isothermal determination of K_{VFT} difficult to be done, a few experiments confirm the tendency of model network-forming mixtures to become less fragile in the course of reaction.[18,24,25]

Second, the α dependence of the glass transition temperature T_g, operationally defined by $\tau(T_g) = 10^2$ s, can be obtained readily from eq 4, once the temperature dependence of $B(T)$ is specified as mentioned above. Evaluating eq 4 for $\tau = 10^2$ s then yields

$$T_g(\alpha) = T_0 + \frac{D \log e}{2 - \log \tau_0}\frac{1}{1 - \langle f\rangle\alpha} \tag{9}$$

This formula should be viewed with caution, as limitations to its validity could arise from the $\Delta C_p \propto 1/T$ assumption (i.e., approximation of the τ behavior vs *T* with a Voghel−Fulcher law)[48] and from limits inherent in the Adam−Gibbs relation, which in the form of eq 4 presumably does not apply to any temperature and extent of reaction. Notwithstanding, it properly reproduces the experimental observation that T_g relates to

conversion in a nonlinear fashion, with T_g rising more sharply with α at high α values.[26,33,40,63,65,68] Also, it is formally equivalent to the semiempirical equations proposed by Pascault and Williams[69] and by Adabbo and Williams[70] to fit experimental $T_g(\alpha)$ data for a variety of thermosets.

A further observation is concerned with the relation between vitrification and gelation phenomena in network-forming systems. In step polymerizations leading to network polymers the critical phenomenon of gelation takes place, which is manifested by shear viscosity (η) tending to infinity,[30] and it is known experimentally that the structural relaxation time does not diverge at the gel point, at which the first network molecule is formed. It has to be noted that eq 4, predicting the divergence of τ when x_n tends to infinity, fully conforms to the observation that gelation precedes the structural arrest of a system, while the extent of reaction at gelation, α_{gel}, corresponds to a relatively low value of x_n. It is possible to calculate approximately the gel point in our systems by applying simple statistical methods. With reference to the Flory's theory,[51] we find an epoxy conversion at gelation of about 0.7, 0.4, and 0.6 in DGEBA348/DETA 4:3, EPON828/EDA 1:1, and EPON828/EDA 2:1 respectively, independent of the temperature. Even if the theory may underestimate α_{gel}, these values are unlikely to change very much: they are significantly lower than the values of α_0 and correspond to x_n of only few units. Also, we did not observe any appreciable change in the characteristics of the d-PCS spectra on crossing the gel point. Insensitivity of the structural relaxation dynamics to gelation is confirmed by dielectric[6,17] and unpolarized PCS measurements[17] and comes out from a different length scale associated with viscous flow and structural relaxation process: the former is a macroscopic length scale, the latter becomes nanometric at the vitrification point. Decoupling of τ and η behaviors in polymerizing systems will be discussed further in future publications.

As a final remark, we note that in Figures 6 and 7 even if the fit was performed only over the range log $(1/\tau_K) > 0$, the same curves are in remarkable agreement with experimental data in a more extended region up to the liquid−glass transition ($\tau_K \approx 10^2$ s). Since determination of these relaxation time data relies on application of the time−conversion superposition principle, as mentioned in section III, this result seems to validate the use of that procedure. The analysis was then extended in DGEBA348/DETA 4:3 to the short correlation-time portion of the spectra collected at very long reaction times. It is observed in Figure 6 that the behavior of τ_K with α seems to depart from the solid line obtained from eq 4, for $\tau_K > 10^2$ s, i.e., when the system enters the glassy state. There, as the reaction proceeds, the slow structural degrees of freedom have not time enough to equilibrate, and the observed behavior might be a nonequilibrium effect. On the other hand, it should be borne in mind that when the reaction is approaching its final stage, the requirements for application of eq 4 tend to become no longer fulfilled.

V. Conclusions

In this work we have used depolarized PCS and calorimetry to monitor several curing processes of three network-forming epoxy−amine formulations that serve as model systems for testing the predictions of a reaction-extended version of the Adam−Gibbs entropy equation. This study demonstrates for the first time the possibility of probing effectively the structural dynamics in epoxy thermosets via collective anisotropy fluctuations.

The relation we provide between structural relaxation time and extent of reaction is supported by the results. Our key ingredient is a connection between the reduction in configurational entropy and the amount of chemical bonds during step polymerization, a quantity that is experimentally accessible. Along the lines described in section II, we also consider the possibility to refine the model equation so as to allow for some departures from ideal assumptions, such as the formation of intramolecular loops: the error due to intramolecular reactions could in principle be reduced by assigning effective functionalities, less than the true stoichiometric ones, to the monomeric reagents, or properly included in the theoretical treatment of number-average properties of a system.

It should be noted that there exist empirical correlations between the change in dynamics and changes in conversion alternative to a Vogel−Fulcher type−Johari and co-workers,[8−10] for example, suggested the relationship $\tau(\alpha) = \tau_0 \exp(S\alpha^p)$ with S and p temperature-dependent parameters characteristic of the polymerization reaction, but no physical basis for such a description was provided. By contrast, the relationship given in eq 4 has a rationale in the Adam and Gibbs model.

As a general implication of the positive test reported here, we find that the dynamics of chemically vitrifying systems is driven by configurational restrictions in a similar way as the dynamics of stable systems undergoing cooling or compression. The energy-landscape formalism[71−73] offers a convenient microscopic perspective for interpreting these findings.[66] Such a similarity strongly suggests that the same mechanism underlies glass formation in physical and chemical vitrification processes, and S_c may become the unifying concept in the physics of systems characterized by slow dynamics, well beyond the restricted world of structural glasses where this concept was introduced. Consistently, we consider that an entropy-based treatment holds the promise of understanding several phenomena in systems such as physical gels, microemulsions, and disordered systems in general, where the dynamics is phenomenologically similar to vitrification.

References and Notes

(1) For a recent review on the liquid−glass transition: Angell, C. A.; Ngai, K. L.; McKenna, G. B.; McMillan, P. F.; Martin, S. W. *J. Appl. Phys.* **2000**, *88*, 3113.
(2) A change of concentration in plasticized systems can also be considered as physical vitrification, as it does not entail forming covalent bonds between the constituent molecules.
(3) Takahara, S.; Yamamuro, O.; Suga, H. *J. Non-Cryst. Solids* **1994**, *171*, 259.
(4) Casalini, R.; Capaccioli, S.; Lucchesi, M.; Rolla, P. A.; Corezzi, S. *Phys. Rev. E* **2001**, *63*, 031207.
(5) Casalini, R.; Capaccioli, S.; Lucchesi, M.; Rolla, P. A.; Paluch, M.; Corezzi, S.; Fioretto, D. *Phys. Rev. E* **2001**, *64*, 041504.
(6) Corezzi, S.; Fioretto, D.; Casalini, R.; Rolla, P. A. *J. Non-Cryst. Solids* **2002**, *307−310*, 281.
(7) Adam, G.; Gibbs, J. H. *J. Chem. Phys.* **1965**, *43*, 139.
(8) Tombari, E.; Ferrari, C.; Salvetti, G.; Johari, G. P. *J. Phys.: Condens. Matter* **1997**, *9*, 7017.
(9) Wasylyshyn, D. A.; Johari, G. P. *J. Polym. Sci., Part B: Polym. Phys.* **1997**, *35*, 437.
(10) Tombari, E.; Salvetti, G.; Johari, G. P. *J. Chem. Phys.* **2000**, *113*, 6957.

(11) Matsuoka, S.; Quan, X.; Bair, H. E.; Boyle, D. J. *Macromolecules* **1989**, *22*, 4093.
(12) Fitz, B.; Mijovic, J. *Macromolecules* **2000**, *33*, 887.
(13) *Dielectric Spectroscopy of Polymeric Materials; Fundamentals and Applications*; Runt, J. P., Fitzgerald, J. J., Eds.; American Chemical Society: Washington, DC, 1997.
(14) *Dielectric Relaxation Spectroscopy; Fundamentals and Applications*; Kremer, F., Schonhals, A., Eds.; Springer: Berlin, 2000.
(15) Bellucci, F.; Valentino, M.; Monetta, T.; Nicodemo, L.; Kenny, J. M.; Nicolais, L.; Mijovic, J. *J. Polym. Sci., Phys. Ed.* **1994**, *32*, 2519.
(16) Williams, G.; Smith, I. K.; Holmes, P. A.; Varma, S. *J. Phys.: Condens. Matter* **1999**, *11*, A57.
(17) Fitz, B. D.; Mijovic, J. *Macromolecules* **1999**, *32*, 4134.
(18) Andjelić, S.; Fitz, B. D.; Mijovic, J. *Macromolecules* **1997**, *30*, 5239.
(19) Johari, G. P.; Ferrari, C.; Tombari, E.; Salvetti, G. *J. Chem. Phys.* **1999**, *110*, 11592.
(20) Cassettari, M.; Salvetti, G.; Tombari, E.; Veronesi, S.; Johari, G. P. *J. Non-Cryst. Solids* **1994**, *172*−*174*, 554.
(21) Levita, G.; Livi, A.; Rolla, P. A.; Culicchi, C. *J. Polym. Sci., Part B: Polym. Phys.* **1996**, *34*, 2731.
(22) Casalini, R.; Corezzi, S.; Fioretto, D.; Livi, A.; Rolla, P. A.*Chem. Phys. Lett.* **1996**, *258*, 470.
(23) Gallone, G.; Capaccioli, S.; Levita, G.; Rolla, P. A.; Corezzi, S. *Polym. Int.* **2001**, *50*, 545.
(24) Parthun, M. G.; Johari, G. P. *J. Chem. Phys.* **1995**, *103*, 440.
(25) Fitz, B.; Andjelić, S.; Mijovic, J. *Macromolecules* **1997**, *30*, 5227.
(26) Schawe, J. E. K. *Thermochim. Acta* **2002**, *391*, 279.
(27) Yamanaka, K.; Inoue, T. *Polymer* **1989**, *30*, 662.
(28) Mangion, M. B. M.; Vanderwal, J. J.; Walton, D.; Johari, G. P. *J. Polym. Sci., Part B: Polym. Phys.* **1991**, *29*, 723 and references therein.
(29) Alig, I.; Lellinger, D.; Nancke, K.; Rizos, A.; Fytas, G. *J. Appl. Polym. Sci.* **1992**, *44*, 829 and references therein.
(30) Matsukawa, M.; Yamura, H.; Nakayama, S.; Otani, T. *Ultrasonics* **2000**, *38*, 466.
(31) Ferrari, C.; Salvetti, G.; Tombari, E.; Johari, G. P. *Phys. Rev. E* **1996**, *54*, R1058.
(32) Schawe, J. E. K.; Alig, I. *Colloid Polym. Sci.* **2001**, *279*, 1169.
(33) Wang, X.; Gillham, J. K. *J. Appl. Polym. Sci.* **1991**, *43*, 2267.
(34) Younes, M.; Wartewig, S.; Lellinger, D.; Strehmel, B.; Strehmel, V. *Polymer* **1994**, *35*, 5269.
(35) Mijovic, J.; Andjelić, S.; Yee, C. F. W.; Bellucci, F.; Nicolais, L. *Macromolecules* **1995**, *28*, 2797.
(36) Apicella, A.; Nicolais, L.; Iannone, M.; Passerini, P. *J. Appl. Polym. Sci.* **1984**, *29*, 2083.
(37) Mijovic, J.; Andjelić, S.; Fitz, B.; Zurawsky, W.; Mondragon, I.; Bellucci, F.; Nicolais, L. *J. Polym. Sci., Part B: Polym. Phys.* **1996**, *34*, 379.
(38) Horie, K.; Hiura, H.; Sawada, M.; Mita, I.; Kambe, H. *J. Polym. Sci., Part A* **1970**, *8*, 1357.
(39) Kenny, J. M.; Trivisano, A. *Polym. Eng. Sci.* **1991**, *31*, 1426.
(40) Jenninger, W.; Schawe, J. E. K.; Alig, I. *Polymer* **2000**, *41*, 1577.
(41) Matsukawa, M.; Okabe, H.; Matsushige, K. *J. Appl. Polym. Sci.* **1993**, *50*, 67.
(42) Berne, B. J.; Pecora, R. *Dynamic Light Scattering*; John Wiley & Sons: New York, 1976.
(43) Patterson, G. D.; Stevens, J. R.; Alms, G. R.; Lindsey, C. P. *Macromolecules* **1979**, *12*, 658.
(44) Patterson, G. D.; Stevens, J. R.; Alms, G. R.; Lindsey, C. P. *Macromolecules* **1979**, *12*, 661.
(45) Chu, B.; Fytas, G. *Macromolecules* **1982**, *15*, 561.
(46) Patterson, G. D.; Lindsey, C. P.; Stevens, J. R. *J. Chem. Phys.* **1979**, *70*, 643.
(47) Kauzmann, W. *Chem. Rev.* **1948**, *43*, 219.
(48) Richert, R.; Angell, C. A. *J. Chem. Phys.* **1998**, *108*, 9016.
(49) Scala, A.; Starr, F. W.; La Nave, E.; Sciortino, F.; Stanley, H. E. *Nature (London)* **2000**, *406*, 166.
(50) Sastry, S. *Nature (London)* **2001**, *409*, 164.
(51) Young, R. J.; Lovell, P. A. *Introduction to Polymers*; Chapman & Hall: New York, 1991.
(52) Stockmayer, W. H. *J. Chem. Phys.* **1943**, *11*, 45.
(53) Macosko, C. W.; Miller, D. R. *Macromolecules* **1976**, *9*, 199.
(54) Kenny, J. M. *J. Appl. Polym. Sci.* **1994**, *51*, 761.
(55) Comez, L.; Fioretto, D.; Palmieri, L.; Verdini, L.; Rolla, P. A.; Gapinski, J.; Pakula, T.; Patkowski, A.; Steffen, W.; Fischer, E. W. *Phys. Rev. E* **1999**, *60*, 3086.
(56) Monaco, G.; Fioretto, D.; Comez, L.; Ruocco, G. *Phys. Rev. E* **2001**, *63*, 061502.
(57) Brodin, A.; Frank, M.; Wiebel, S.; Shen, G.; Wuttke, J.; Cummins, H. Z. *Phys. Rev. E* **2002**, *65*, 051503.
(58) Lunak, S.; Dusek, K. *J. Polym. Sci., Polym. Symp. Ed.* **1975**, *53*, 45.
(59) Flory, P. J. *J. Phys. Chem. Soc.* **1942**, *46*, 132.
(60) (a) Flory, P. J. *J. Am. Chem. Soc.* **1941**, *63*, 3083. (b) **1941**, *63*, 3091. (c) **1941**, *63*, 3096.
(61) Gordon, M. *Proc. R. Soc. London, Ser. A* **1962**, *268*, 240.
(62) Miller, D. R.; Macosko, C. W *Macromolecules* **1978**, *11*, 656.
(63) Enns, J. B.; Gillham, J. K. *J. Appl. Polym. Sci.* **1983**, *28*, 2567.
(64) Golub, M. A.; Lerner, N. R. *J. Appl. Polym. Sci.* **1986**, *32*, 5215.
(65) Wise, C. W.; Cook, W. D.; Goodwin, A. A. *Polymer* **1997**, *38*, 3251 and references therein.
(66) Corezzi, S.; Fioretto, D.; Rolla, P. *Nature (London)* **2002**, *420*, 653.
(67) Angell, C. A. *J. Non-Cryst. Solids* **1991**, *131*−*133*, 13.
(68) Simpson, J. O.; Bidstrup, S. A. *J. Polym. Sci., Part B* **1995**, *33*, 53.
(69) Pascault, J. P.; Williams, R. J. J. *J. Polym. Sci., Polym. Phys.* **1990**, *28*, 85.
(70) Adabbo, H. E.; Williams, R. J. J. *J. Appl. Polym. Sci.* **1982**, *27*, 1327.
(71) Goldstein, M. *J. Chem. Phys.* **1969**, *51*, 3728.
(72) Stillinger, F. H. *Science* **1995**, *267*, 1935.
(73) Sastry, S.; Debenedetti, P. G.; Stillinger, F. H. *Nature (London)* **1998**, *393*, 554.

MA026021Q